ELSEVIER

Available online at www.sciencedirect.com
SCIENCE DIRECT®

Fluid Dynamics Research 36 (2005) 319–332

FLUID DYNAMICS RESEARCH

Inflexional disequilibrium of magnetic flux-tubes

Renzo L. Ricca[a, b, *]

[a] *Department of Mathematics and Applications, Università di Milano-Bicocca, Via Cozzi 53, Milano 20125, Italy*
[b] *Department of Mathematics, University College London, Gower Street, London WC1E 6BT, UK*

Received 23 March 2004; received in revised form 21 August 2004; accepted 27 September 2004

Communicated by S. Kida

In memory of Richard Pelz, colleague and friend

Abstract

In this paper, we prove that magnetic flux-tubes in inflexional configuration are in disequilibrium and evolve to an inflexion-free state. The magnetic field is defined in a tube of circular cross-section and is chosen so as to have toroidal and poloidal components contributing to the internal twist of the flux-tube. By using orthogonal curvilinear coordinates, we derive the equations for the Lorentz force associated with the magnetic flux-tube and use them to study the generic behaviour associated with passage through inflexional configuration. Inflexional state is attained when local curvature vanishes as the tube axis changes concavity. We check that the conditions for the equilibrium of the flux-tube in inflexional configuration are not satisfied and hence we prove disequilibrium. Inflexional disequilibrium makes magnetic flux-tubes evolve to an inflexion-free state. As a consequence, inflexional flux-tubes in free space evolve naturally to an inflexion-free configuration. This mechanism has important implications for the energetics of solar coronal loops and astrophysical flows.

PACS: 03.40.Gc; 47.65.+a; 02.40.+m

Keywords: Magnetic flux-tube; Lorentz force; Topological fluid mechanics; Inflexional geometry; Magnetic energy

* Department of Mathematics and Applications, Università di Milano-Bicocca, Via Cozzi 53, Milano 20125, Italy. Tel.: +39 026448 5762; fax: +39 026448 5705.
E-mail address: renzo.ricca@unimib.it.

0169-5983/$30.00
doi:10.1016/j.fluiddyn.2004.09.004

1. Introduction

In this paper, we prove that magnetic flux-tubes in inflexional configuration are in disequilibrium and evolve to an inflexion-free state. The magnetic flux-tube is given by a thin, cylindrical tube with prescribed magnetic field and twist. The flux-tube is supposed to be in isolation and embedded in ideal fluid (no dissipation). By using new equations for the Lorentz force in orthogonal curvilinear coordinates, we study the conditions for equilibrium associated with passage through inflexional configuration. This configuration is attained when the curvature of the tube axis vanishes and there is a change in concavity of the tube geometry. We prove that when a magnetic flux-tube is in inflexional geometry, then there is local disequilibrium. Inflexional disequilibrium is due to the presence of a rotational flow that forces the tube strand to remove inflexion, hence deforming the tube to an inflexion-free configuration. Since the evolution is in ideal conditions, topology is conserved; hence, disequilibrium induces a deformation governed by a diffeomorphism of the ambient space, that maps the inflexional magnetic flux-tube to an inflexion-free configuration. This mechanism has important consequences for the re-distribution of magnetic energy, and writhe and twist helicity (Moffatt and Ricca, 1992; Chui and Moffatt, 1996). It is therefore important for the study of energetics of plasma loops in the solar corona, in astrophysical flows and laboratory plasmas.

It is well-known that solar coronal loops are basic structural elements of solar and stellar atmospheres (Bray et al., 1991). On the Sun, more than 90% of the magnetic flux outside sunspots is concentrated into localized flux-tubes, that are responsible for a great part of energy emission from the solar corona. The existence of truly complex magnetic field topologies, with lines of force highly twisted and braided, makes it difficult to estimate the energy stored in these structures. In recent years, thanks to a combined use of new mathematical concepts and advanced numerical simulation, there has been growing interest to study energetic and dynamical aspects of complex structures by using geometric and topological methods (Ricca, 2001). In the study of magnetic flux-tubes, for instance, these methods have been particularly successful (Berger and Field, 1984; Moffatt and Ricca, 1992; Ricca and Berger, 1996). As has been shown by Ricca (1994, 1997), geometries characterized by spontaneous formation of hammock configurations, braided structures and dynamical features typical of solar coronal loops can be related to the appearance and disappearance of inflexional states. Inflexional configurations are like bifurcation points of flows in dynamical systems: according to the physical parameters involved their appearance may trigger quite different dynamics; it is therefore important to establish whether conditions for possible equilibria exist or not.

Inflexional geometries may appear ubiquitously in plasma loops and magnetic structures that form complex topologies. In astrophysical context, though, plasma loops are more likely to form highly braided patterns organized in gigantic arches (with a dominant concave region), rather than being convoluted in knotted configurations, with lots of regions of opposite concavity. This suggests that inflexional geometries, rare in braids, but certainly dense in magnetic knots, are states of magnetic disequilibrium.

Inflexional states also play an important role in the formation of hammock configurations. These states are formed when cool plasma, heavier than the surrounding fluid, sits on a magnetic arch. Depending on the value of local parameters, including magnetic field twist, a magnetic structure in a hammock shape may form to sustain cool plasma in the upper atmosphere. At appropriately high twist values, it is possible to show (Ricca, 1994) that inflexional geometry may emerge as a result of the delicate equilibrium between (mainly) mechanical and magnetic forces. In this case, an inflexional disequilibrium would help to trigger the break-up of magnetic structure (erupting plasma loop), with immediate release of part of the energy

stored in the system. Alternatively, at low twist values, inflexional disequilibrium would simply drive an internal re-distribution of magnetic energy, with some exchange of twist helicity into writhe helicity. Thus, spontaneous development of inflexional configurations may play an important role in the energy relaxation of solar coronal loops and magnetic field topologies.

In the next Section 2, we introduce a flux-tube model, by prescribing geometry and magnetic field distribution. The magnetic field is chosen so as to have toroidal and poloidal components contributing to the internal twist of the flux-tube. In Section 3, by using an appropriate system of orthogonal, curvilinear coordinates, we derive the equations for the Lorentz force associated with the flux-tube. Generic passage through inflexional configuration is briefly discussed in Section 4. In Section 5, we prove our main result, that magnetic flux-tubes in inflexional configuration are in disequilibrium. The proof is based on three steps: first, we derive the conditions for magnetostatic equilibrium, then we apply these conditions to inflexional geometry; finally, we prove disequilibrium. In Section 6, as a corollary of this result, we show that flux-tubes in inflexional configuration are naturally led to evolve to inflexion-free states, by re-arranging local geometry and magnetic field distribution.

2. Magnetic flux-tube with twist

In this section, we define a magnetic flux-tube $\mathscr{K}_{\rm m}$ as a standard embedding in an ideal fluid in $\mathscr{D} \subseteq \mathbb{R}^3$. The tube axis $\mathscr{C}$ is a simple, smooth curve in $\mathbb{R}^3$ of length L and vector equation $\mathbf{x} = \mathbf{X}(s)$, where s denotes arc-length on $\mathscr{C}$, with $s = 0$ at some origin O. The tube $\mathscr{T} \equiv \mathscr{S} \otimes \mathscr{C}$ has circular cross-section $\mathscr{S}$, of area $A = \pi a^2$, and we assume a to be small compared with the local radius of curvature R of $\mathscr{C}$. The tube thickness, which is the inverse of the tube aspect ratio, is given by a/R. Deviations from cylindrical geometry are neglected and regarded as effects of higher-order.

Let (r, ϑ_R, s) be orthogonal, curvilinear coordinates centred on $\mathscr{C}$ (Mercier, 1963). A point P on $\mathscr{S}$ (see Fig. 1a) is given by

$$\mathbf{x} = \mathbf{X}(s) + r\cos\vartheta(s)\hat{\mathbf{n}}(s) + r\sin\vartheta(s)\hat{\mathbf{b}}(s), \tag{1}$$

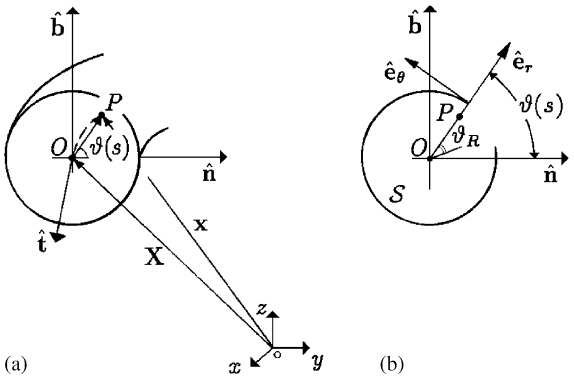

Fig. 1. (a) Relationship between fixed and moving frame for a point P on $\mathscr{S}$: the angle $\vartheta(s)$ varies with the torsion of $\mathscr{C}$. (b) Frenet pair $(\hat{\mathbf{n}}, \hat{\mathbf{b}})$ and unit vectors $(\hat{\mathbf{e}}_r, \hat{\mathbf{e}}_\theta)$ in the cross-section $\mathscr{S}$ of $\mathscr{T}$.

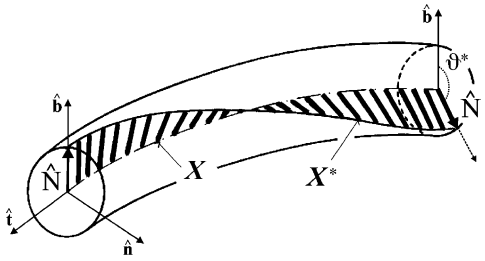

Fig. 2. Twist of field lines may be visualized by means of a ribbon, whose edges are given by the tube axis $\mathbf{X} = \mathbf{X}(s)$ and a neighbouring curve $\mathbf{X}^*$, placed at a distance r in the spanwise direction $\hat{\mathbf{N}}$ on the ribbon relative to the Frenet pair $(\hat{\mathbf{n}}, \hat{\mathbf{b}})$.

where $\vartheta(s)$ is the polar angle referred to the unit normal $\hat{\mathbf{n}} = \hat{\mathbf{n}}(s)$ in the intrinsic reference frame (Frenet frame), given by unit tangent $\hat{\mathbf{t}} = \hat{\mathbf{t}}(s) \equiv \mathrm{d}\mathbf{x}/\mathrm{d}s$, normal $\hat{\mathbf{n}}$ and binormal $\hat{\mathbf{b}} = \hat{\mathbf{b}}(s)$ to $\mathscr{C}$. This angle varies according to the geometry of the tube-axis. The polar angle ϑ_R, however, is an independent coordinate and is related to the former by the equation

$$\vartheta(s) = \vartheta_R + \gamma(s), \tag{2}$$

where

$$\gamma(s) = -\int_0^s \tau(\xi)\,\mathrm{d}\xi \tag{3}$$

takes into account the contribution from the torsion $\tau = \tau(s)$ of $\mathscr{C}$. By using Frenet–Serret formulae

$$\hat{\mathbf{t}}' = c\hat{\mathbf{n}}, \quad \hat{\mathbf{n}}' = -c\hat{\mathbf{t}} + \tau\hat{\mathbf{b}}, \quad \hat{\mathbf{b}}' = -\tau\hat{\mathbf{n}}, \tag{4}$$

where $c = c(s)$ is curvature ($c \equiv R^{-1}$) and prime denotes derivative with respect to s, we define the metric

$$\mathrm{d}\mathbf{x} \cdot \mathrm{d}\mathbf{x} = (\mathrm{d}r)^2 + r^2(\mathrm{d}\vartheta_R)^2 + K^2(\mathrm{d}s)^2, \tag{5}$$

which is orthogonal; here $K = K(s) = 1 - c(s)r\cos\vartheta(s)$. The orthogonal basis $(\hat{\mathbf{e}}_r, \hat{\mathbf{e}}_\theta, \hat{\mathbf{t}})$ is given by $\hat{\mathbf{e}}_r = \hat{\mathbf{n}}\cos\vartheta + \hat{\mathbf{b}}\sin\vartheta$, $\hat{\mathbf{e}}_\theta = -\hat{\mathbf{n}}\sin\vartheta + \hat{\mathbf{b}}\cos\vartheta$ and $\hat{\mathbf{t}}$, in the radial, meridian and longitudinal direction, respectively (see Fig. 1b).

We want to consider magnetic flux-tubes with twist, that is with field lines wound about the tube axis in the longitudinal direction. Twist can be easily visualized by means of a ribbon (see Fig. 2), whose edges are the tube axis $\mathbf{X} = \mathbf{X}(s)$ and a neighbouring curve $\mathbf{X}^*(s) = \mathbf{X}(s) + r\hat{\mathbf{N}}(s)$, placed at a distance r in the spanwise direction given by the unit vector $\hat{\mathbf{N}} = \hat{\mathbf{n}}\cos\vartheta^* + \hat{\mathbf{b}}\sin\vartheta^*$ on the ribbon relative to the Frenet pair $(\hat{\mathbf{n}}, \hat{\mathbf{b}})$. The winding of $\mathbf{X}^*$ around $\mathscr{C}$ is measured by the total twist number Tw for a ribbon, given by (Fuller, 1971)

$$Tw = \frac{1}{2\pi}\oint_{\mathscr{C}} (\hat{\mathbf{N}}' \times \hat{\mathbf{N}}) \cdot \hat{\mathbf{t}}\,\mathrm{d}s. \tag{6}$$

By using the Frenet–Serret equations (4), we have

$$\hat{\mathbf{N}}' = \frac{\mathrm{d}\hat{\mathbf{N}}}{\mathrm{d}s} = -c\cos\vartheta^*\,\hat{\mathbf{t}} + (\tau + \mathrm{d}\vartheta^*/\mathrm{d}s)\hat{\mathbf{e}}_\theta. \tag{7}$$

Hence, by Eq. (6), the total twist for a ribbon is given by

$$Tw = \frac{1}{2\pi}\oint_{\mathscr{C}} (\hat{\mathbf{N}}' \times \hat{\mathbf{N}}) \cdot \hat{\mathbf{t}}\, \mathrm{d}s = \frac{1}{2\pi}\oint_{\mathscr{C}} \tau\, \mathrm{d}s + \frac{1}{2\pi}[\vartheta^*]_{\mathscr{C}}, \tag{8}$$

where the integral on the l.h.s. of the equation is the total torsion of $\mathscr{C}$ and the last term is an integer representing the number of rotations of $\hat{\mathbf{N}}$ in one passage round $\mathscr{C}$.

The magnetic field $\mathbf{B}$ is non-zero in $\mathscr{T}$ and is identically zero in $(\mathscr{D} - \mathscr{T})$. For simplicity, we consider the field decomposition given by

$$\mathbf{B} = \mathbf{B}_{\mathrm{m}} + \mathbf{B}_{\mathrm{a}}, \tag{9}$$

with $\mathbf{B}_{\mathrm{m}} = B_\theta \hat{\mathbf{e}}_\theta$ the meridian (poloidal) component in $\mathscr{S}$ and $\mathbf{B}_{\mathrm{a}} = B_s \hat{\mathbf{t}}$ the longitudinal (toroidal) component along $\mathscr{C}$. The field is chosen so as to have no radial component, so that the tube boundary is a magnetic surface ($\mathbf{B} \cdot \hat{\mathbf{N}} = 0$). We take

$$\mathbf{B}_{\mathrm{m}} = [0,\, B_\theta(r, \vartheta(s)), 0], \quad \mathbf{B}_{\mathrm{a}} = [0, 0,\, B_s(r)], \tag{10}$$

where everything is a smooth function of radius and arc-length. Since $\mathbf{B}$ is divergenceless, we have

$$r\nabla \cdot \mathbf{B} = \frac{\partial B_\theta}{\partial \vartheta_R} + B_\theta \frac{cr}{K} \sin\vartheta + \frac{r}{K}\frac{\partial B_s}{\partial s} = 0. \tag{11}$$

From the second of (10), we have $\partial B_s/\partial s = 0$, so that (11) reduces to

$$\frac{\partial B_\theta}{\partial \vartheta_R} = -B_\theta \frac{cr}{K} \sin\,\vartheta, \tag{12}$$

a relation that will be used below to derive the Lorentz force.

It is worth mentioning the special case of *uniform* twist. From the definition of magnetic line, we have

$$\frac{r\,\delta\vartheta_R}{B_\theta} = \frac{K\,\delta s}{B_s}. \tag{13}$$

In case of uniform twist, we must have

$$\frac{\delta\vartheta_R}{\delta s} = \frac{\oint_{\mathscr{C}} \mathrm{d}\vartheta_R}{\oint_{\mathscr{C}} \mathrm{d}s} = \frac{2\pi T w}{L}. \tag{14}$$

Hence, by using Eq. (13), we have

$$2\pi T w = \frac{KL}{r}\frac{B_\theta}{B_s}, \tag{15}$$

that puts in relation geometric and magnetic quantities. From this equation, we note that the condition of uniform twist implies $B_\theta/B_s \approx r$, that poses a restriction on the relationship between toroidal and poloidal components of the magnetic field.

3. Lorentz force associated with magnetic flux-tube

The Lorentz force is given by $\mathbf{F} = \mathbf{J} \times \mathbf{B}$, where $\mathbf{J}$ is the current density. Since $\mathbf{J} = \nabla \times \mathbf{B}$, we have:

$$\mathbf{F} = (\nabla \times \mathbf{B}) \times \mathbf{B} = (\mathbf{B} \cdot \nabla)\mathbf{B} - \tfrac{1}{2}\nabla(\mathbf{B}^2). \tag{16}$$

The r.h.s. of this equation can be made explicit in terms of the magnetic field prescribed. By using (9), the first of (4) and (10), we have

$$(\mathbf{B} \cdot \nabla)\mathbf{B} = \frac{B_\theta^2}{r}\frac{\partial \hat{\mathbf{e}}_\theta}{\partial \vartheta_R} + \left(\frac{B_\theta}{r}\frac{\partial B_\theta}{\partial \vartheta_R} + \frac{B_s}{K}\frac{\partial B_\theta}{\partial s}\right)\hat{\mathbf{e}}_\theta + \frac{B_\theta B_s}{K}\frac{\partial \hat{\mathbf{e}}_\theta}{\partial s} + \frac{B_s^2}{K}c\hat{\mathbf{n}}. \tag{17}$$

By (2) and (3), we have

$$\frac{\partial B_\theta}{\partial s} = \frac{\partial B_\theta}{\partial \vartheta}\bigg|_s \frac{\partial \vartheta}{\partial s} = \frac{\partial B_\theta}{\partial \vartheta_R}\bigg|_s \frac{\partial \gamma}{\partial s} = -\tau\frac{\partial B_\theta}{\partial \vartheta_R}, \tag{18}$$

so that by (12), we have

$$\frac{\partial B_\theta}{\partial s} = B_\theta \frac{cr\tau}{K}\sin\vartheta. \tag{19}$$

Eq. (17) reduces to

$$(\mathbf{B} \cdot \nabla)\mathbf{B} = B_s^2\frac{c}{K}\hat{\mathbf{n}} - \frac{B_\theta^2}{r}\hat{\mathbf{e}}_r + B_\theta\frac{c}{K}\sin\vartheta\left(B_s\frac{r\tau}{K} - B_\theta\right)\hat{\mathbf{e}}_\theta + B_\theta B_s\frac{c}{K}\sin\vartheta\hat{\mathbf{t}}. \tag{20}$$

Similarly for the second term in the r.h.s. of (16):

$$\frac{1}{2}\nabla(\mathbf{B}^2) = \frac{1}{2}\left[\frac{\partial}{\partial r}(B_\theta^2 + B_s^2)\hat{\mathbf{e}}_r - 2B_\theta^2\frac{c}{K}\sin\vartheta\hat{\mathbf{e}}_\theta + 2B_\theta^2\frac{cr\tau}{K^2}\sin\vartheta\hat{\mathbf{t}}\right]. \tag{21}$$

Substituting (20) and (21) into (16), we have $\mathbf{F} = \mathbf{F}_r + \mathbf{F}_m + \mathbf{F}_a$, where

$$\mathbf{F}_r = F_r\hat{\mathbf{e}}_r = \left[B_s^2\frac{c}{K}\cos\vartheta - \frac{B_\theta^2}{r} - \frac{1}{2}\frac{\partial}{\partial r}(B_\theta^2 + B_s^2)\right]\hat{\mathbf{e}}_r, \tag{22}$$

$$\mathbf{F}_m = F_\theta\hat{\mathbf{e}}_\theta = B_s\frac{c}{K}\sin\vartheta\left(B_\theta\frac{r\tau}{K} - B_s\right)\hat{\mathbf{e}}_\theta, \tag{23}$$

$$\mathbf{F}_a = F_s\hat{\mathbf{t}} = B_\theta\frac{c}{K}\sin\vartheta\left(B_s - B_\theta\frac{r\tau}{K}\right)\hat{\mathbf{t}}, \tag{24}$$

are the components of the Lorentz force $\mathbf{F}$ in the orthogonal coordinates (r, ϑ_R, s). In physical applications, it is customary to combine radial and meridian components in two contributions, one given by $\mathbf{F}_\perp$, perpendicular to the tube axis, and one given by $\mathbf{F}_p$, in the meridian plane:

$$\mathbf{F}_\perp = B_s^2\frac{c}{K}\hat{\mathbf{n}} - \left[\frac{B_\theta^2}{r} + \frac{1}{2}\frac{\partial}{\partial r}(B_\theta^2 + B_s^2)\right]\hat{\mathbf{e}}_r, \tag{25}$$

$$\mathbf{F}_p = B_\theta B_s\frac{cr\tau}{K^2}\sin\vartheta\hat{\mathbf{e}}_\theta. \tag{26}$$

Evidently this decomposition is not unique, because now the term in $\hat{\mathbf{n}}$ includes part of the contribution in $\hat{\mathbf{e}}_\theta$. However, Eqs. (25) and (26) help to understand the dynamics associated with the Lorentz force: the magnetic flux-tube moves in the fluid thanks to the action of $\mathbf{F}_\perp$, with a term proportional to curvature along the principal normal, corrected by the scale factor K, and a term in the radial direction, that takes account of magnetic pressure. The curvature term is responsible for the natural shortening of flux-tubes in free space, and contributes to the bending energy of the magnetic tube, in analogy with elastic systems. The radial term controls the confinement of the magnetic field in the tubular region, through the magnetic pressure generated by the poloidal and toroidal components of $\mathbf{B}$. Note that for relatively thick flux-tubes, the scale factor $K = 1 - cr\cos\vartheta$ may enhance considerably the curvature force.

The contributions $\mathbf{F}_a$ and $\mathbf{F}_p$ induce internal re-organization of the magnetic field, without affecting the shape of the flux-tube; the axial component $\mathbf{F}_a$ contributes to internal stretching and generates longitudinal magnetic tension in $\mathscr{T}$, while the poloidal component (26) induces a meridian flow around the tube cross-section, that brings fluid from the concave to the convex region of the tube, hence modifying the twist distribution of the field-lines. In case of uniform twist (see condition (14)), by using Eq. (15) we have

$$\frac{|\mathbf{F}_a|}{|\mathbf{F}_m|} = -\frac{B_\theta}{B_s} = -\frac{2\pi T w}{L}\frac{r}{K}. \tag{27}$$

4. Generic behaviour associated with inflexional configuration

Inflexional configurations are characterized by the presence of points of inflexions, where local curvature vanishes as the tube axis changes concavity. Inflexional geometries are easily identifiable in plane curves, when these have an S-shape (see Fig. 3a). More generally, inflexional states may appear in the evolution of flux-tubes when, for example, loops are produced from hammock configurations (see Fig. 3b). It should be stressed that inflexional geometry is an intrinsic property of a curve, and does not depend on the projection. Ricca and Moffatt (1992) proposed an intrinsic kinematic model to describe

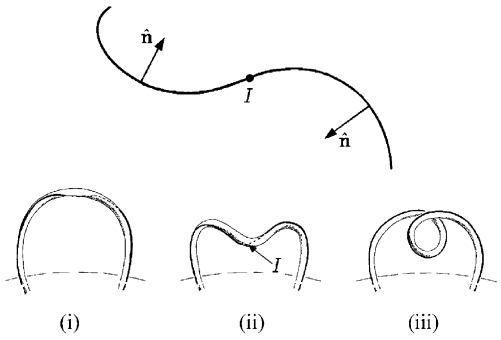

Fig. 3. (a) Inflexional geometry in a plane curve: the point of inflexion I, defined by $c = 0$, is located where the curve changes concavity. (b) Example of passage through an inflexional configuration during the evolution of flux-tubes: the process may start from an arch-like configuration, as in (i), to end with a loop formation (iii) through a Reidemeister type I move. The appearance of an inflexional state (ii) is invariably associated with the exchange of writhe and twist during the process.

the generic behaviour associated with passage through inflexional configuration. This model was used to analyse exchange of writhe and twist in magnetic helicity (Moffatt and Ricca, 1992) and to study relaxation to hammock configurations of solar coronal loops (Ricca, 1994). Here we recall some basic results necessary to prove the statement of next section.

A flux-tube is said to be in inflexional configuration when $\mathbf{x} = \mathbf{X}(s)$ has at least one point of inflexion, say at $s = s_c$. We assume that the inflexion point is in isolation: by definition, this means that $c(s_c) = 0$. We may therefore choose to re-position the origin O at the inflexion point, where $s = s_c = 0$, and axes $Oxyz$ with Ox parallel to $\hat{\mathbf{t}}(s_c)$ and Oz parallel to $\hat{\mathbf{t}}''$. By a Taylor's expansion near $s = s_c$ and by simple re-scaling, we find (Ricca and Moffatt, 1992) that the generic shape of an inflexional geometry is given by the cubic curve

$$\mathbf{X}(s) = (s, 0, s^3). \tag{28}$$

Note that this is an intrinsic description, independent of the external reference and parametrization.

The emergence of an inflexional state and generic passage through inflexion can be described by an intrinsic kinematic model. This can be encapsulated in a time-dependent curve $\mathbf{x}=\mathbf{X}(s, t)$ passing through the inflexional configuration (28) at $t = 0$, but having $\partial\hat{\mathbf{t}}/\partial s \neq 0$ when $t \neq 0$. Since

$$\hat{\mathbf{t}}' \cdot \hat{\mathbf{t}} = \frac{1}{2}\frac{\partial(\hat{\mathbf{t}}^2)}{\partial s} = 0, \tag{29}$$

we may always, by rigid rotation, ensure that at $s = 0$, $\hat{\mathbf{t}}$ remains parallel to Ox and $\hat{\mathbf{t}}'$ remains parallel to Oy. These conditions are satisfied (generically) by the time-dependent twisted cubic

$$\mathbf{X}(s, t) = (s - \tfrac{2}{3}t^2 s^3, -ts^2, s^3), \tag{30}$$

for which

$$\hat{\mathbf{t}} = \partial\mathbf{X}/\partial s = (1 - 2t^2 s^2, -2ts, 3s^2), \tag{31}$$

so that, near $s = 0$, we have $|\hat{\mathbf{t}}| = 1 + O(s^4)$, which is indeed the unit tangent vector. Here time is simply a kinematic parameter and it can change sign according to the appearance or disappearance of inflexional geometry. Eq. (30) can be used to mimic Reidemeister type I move, to model exchange of writhe and twist helicity under conservation of linking number (see Moffatt and Ricca, 1992). By using the Frenet–Serret Eqs. (4), from (30) we have (to leading order in $|s|$ and $|t|$) curvature and torsion, given by

$$c(s, t) \sim 2(t^2 + 9s^2)^{1/2}, \quad \tau(s, t) \sim \frac{-3t}{t^2 + 9s^2}. \tag{32}$$

Note that c vanishes only at $t = s = 0$, and τ is singular at the inflexion point. The singularity, however, is integrable and the contribution to $\gamma(s)$ (see Eq. (3)) from a small interval $[0, s]$ is given by

$$\gamma(s) = -\int_0^s \tau(\xi)\,\mathrm{d}\xi = \int_0^s \frac{3t}{t^2 + 9\xi^2}\,\mathrm{d}\xi = \arctan\left(\frac{3s}{t}\right), \tag{33}$$

where $s \gg |t|$.

5. Inflexional disequilibrium of magnetic flux-tubes

We prove the following result:

Theorem. *Let $\mathscr{K}_m \hookrightarrow \mathscr{D}$ be the standard embedding of a magnetic flux-tube in $\mathscr{D}$, with magnetic field defined by Eqs.* (9) *and* (10). *Let $\tilde{\mathscr{K}}_{m,t}$ denote the generic, time-dependent passage of $\mathscr{K}_m$ through inflexional configuration. Then, the magnetic flux-tube $\tilde{\mathscr{K}}_{m,t}$ is in inflexional disequilibrium.*

The proof of this result is based on three steps: (i) we derive the conditions for equilibrium for $\mathscr{K}_m$; (ii) we apply these conditions to study the generic passage through an inflexion point; (iii) we examine these conditions and prove inflexional disequilibrium.

Proof. (i) *Conditions for equilibrium*: In absence of background flow, magnetostatic equilibrium is ensured by having irrotational flow in the meridian plane, or, equivalently by the condition $\mathbf{J} \times \mathbf{B} = \nabla p$ (p pressure). From the momentum equation equilibrium is thus given by

$$\nabla \times \mathbf{F} = 0. \tag{34}$$

By using the orthogonal metric (5), we have

$$(\nabla \times \mathbf{F})_r = (rK)^{-1}[\partial(KF_s)/\partial\vartheta_R - \partial(rF_\theta)/\partial s], \tag{35}$$
$$(\nabla \times \mathbf{F})_\theta = (K)^{-1}[\partial F_r/\partial s - \partial(KF_s)/\partial r], \tag{36}$$
$$(\nabla \times \mathbf{F})_s = (r)^{-1}[\partial(rF_\theta)/\partial r - \partial F_r/\partial\vartheta_R]. \tag{37}$$

By using the Lorentz force components (22)–(24) associated with the magnetic field decomposition (10), we can work out Eqs. (35)–(37) explicitly. After some tedious but straightforward algebra, the equilibrium conditions expressed by (34) are given by

$$\begin{aligned}(\nabla \times \mathbf{F})_r = {} & B_\theta B_s \left\{ c\left(\cos\vartheta - \frac{cr}{K}\sin^2\vartheta\right) - \frac{r^2}{K^2}\left[3\frac{c^2 r\tau^2}{K}\sin^2\vartheta \right.\right. \\ & \left.\left. + \; c'\tau\sin\vartheta\left(1 + 2\frac{cr}{K}\cos\vartheta\right) + c(\tau'\sin\vartheta - \tau^2\cos\vartheta)\right]\right\} \\ & + B_\theta^2\frac{cr\tau}{K}\left(3\frac{cr}{K}\sin^2\vartheta - \cos\vartheta\right) + B_s^2\frac{r}{K} \\ & \times\left[c'\sin\vartheta\left(1 + \frac{cr}{K}\cos\vartheta\right) + c\tau\left(\frac{cr}{K}\sin^2\vartheta - \cos\vartheta\right)\right] = 0,\end{aligned} \tag{38}$$

$$\begin{aligned}(\nabla \times \mathbf{F})_\theta = {} & \frac{B_s^2}{K}\left(1 + \frac{cr}{K}\cos\vartheta\right)(c'\cos\vartheta + c\tau\sin\vartheta) - 2B_\theta^2\frac{c\tau}{K}\sin\vartheta \\ & - \frac{\partial}{\partial r}(B_\theta B_s)c\sin\vartheta = 0,\end{aligned} \tag{39}$$

and

$$\begin{aligned}(\nabla \times \mathbf{F})_s = {} & \frac{B_\theta^2}{r}\left(3 + \frac{cr}{K}\cos\vartheta\right) - 2B_\theta B_s\frac{\tau}{K}\left(1 + \frac{cr}{K}\cos\vartheta\right) \\ & - \frac{\partial}{\partial r}(B_\theta B_s)\frac{r\tau}{K} + \frac{\partial}{\partial r}(B_\theta^2 + B_s^2) = 0.\end{aligned} \tag{40}$$

(ii) *Passage through inflexion point*: Generic passage through inflexional configuration is given by Eq. (30), with curvature and torsion changing according to (32). In order to have non-dimensional quantities, we normalize arc-length with respect to a reference length ρ_c (chosen so as to be of order of c^{-1} near s_c), that is $\hat{s} = s/\rho_c$. Since $\partial/\partial s = \rho_c^{-1}\partial/\partial\hat{s}$, Eqs. (32) become

$$c(\hat{s}, t) \sim \frac{1}{\rho_c} f_c(\hat{s}, t), \quad \tau(\hat{s}, t) \sim \frac{1}{\rho_\tau} f_\tau(\hat{s}, t), \tag{41}$$

where

$$f_c(\hat{s}, t) = 2(t^2 + 9\hat{s}^2)^{1/2}, \quad f_\tau(\hat{s}, t) = \frac{-3t}{t^2 + 9\hat{s}^2}, \tag{42}$$

and ρ_τ is a reference length of order of τ^{-1} near s_c. We have

$$cr = \frac{r}{\rho_c} f_c = \varepsilon f_c, \quad \tau r = \frac{r}{\rho_\tau} f_\tau = \varepsilon\eta f_\tau, \tag{43}$$

where $\eta = \rho_c/\rho_\tau = O(1)$. In plane geometry, we have $\tau = 0$ and $\eta = 0$.

Conditions for inflexional equilibrium are determined by substituting (41)–(43) into Eqs. (38)–(40). Since a local change δr does not alter the value of c and τ, ρ_c and ρ_τ remain constant; since $\varepsilon = r/\rho_c$ (cf. Eqs. (43) above), we have $\delta r = \rho_c \delta\varepsilon$ and therefore $\partial/\partial r \equiv (\rho_c)^{-1}\partial/\partial\varepsilon$. After some more algebra, we must ensure that the following system of three equations is satisfied simultaneously:

$$B_\theta^2 \tilde{A} + B_s^2 \tilde{B} + B_\theta B_s \tilde{C} = 0, \tag{44}$$

$$B_\theta^2 \tilde{D} + B_s^2 \tilde{E} + \frac{\partial}{\partial\varepsilon}(B_\theta B_s)\tilde{F} = 0, \tag{45}$$

$$B_\theta^2 \tilde{G} + B_\theta B_s \tilde{H} + \frac{\partial}{\partial\varepsilon}(B_\theta B_s)\tilde{I} + \frac{\partial}{\partial\varepsilon}(B_\theta^2 + B_s^2)\tilde{J} = 0, \tag{46}$$

where $\tilde{A}, \tilde{B}, \ldots, \tilde{J}$ are smooth functions of $\{\hat{s}, t, \vartheta_R;\ \varepsilon, \eta\}$.

The functions in (44) are given by

$$\tilde{A} = \varepsilon\frac{\eta f_c f_\tau}{K}\left(3\frac{\varepsilon f_c}{K}\sin^2\vartheta - \cos\vartheta\right), \tag{47}$$

$$\tilde{B} = \frac{\varepsilon}{K}\left[\frac{18\hat{s}}{b^{1/2}}\sin\vartheta\left(\frac{\varepsilon f_c}{K}\cos\vartheta + 1\right) + \eta f_c f_\tau\left(\frac{\varepsilon f_c}{K}\sin^2\vartheta - \cos\vartheta\right)\right], \tag{48}$$

$$\tilde{C} = f_c\left(\cos\vartheta - \frac{\varepsilon f_c}{K}\sin^2\vartheta\right) - \frac{\varepsilon^2}{K^2}\left[3\frac{\varepsilon\eta^2 f_c^2 f_\tau^2}{K}\sin^2\vartheta + \frac{18\hat{s}}{b^{1/2}}\eta f_\tau\sin\vartheta \times\left(1 + 2\frac{\varepsilon f_c}{K}\cos\vartheta\right) + \eta f_c\left(\frac{54t\hat{s}}{b^2}\sin\vartheta - \eta f_\tau^2\cos\vartheta\right)\right]; \tag{49}$$

the functions in (45) are given by

$$\tilde{D} = -2\frac{\eta f_c f_\tau}{K}\sin\vartheta, \tag{50}$$

$$\tilde{E} = \frac{1}{K}\left(\frac{18\hat{s}}{b^{1/2}}\cos\vartheta + \eta f_c f_\tau\sin\vartheta\right)\left(1 + \frac{\varepsilon f_c}{K}\cos\vartheta\right), \tag{51}$$

$$\tilde{F} = -f_c\sin\vartheta; \tag{52}$$

and the functions in (46) are given by

$$\tilde{G} = 3 + \frac{\varepsilon f_c}{K}\cos\vartheta, \quad \tilde{H} = -2\varepsilon\frac{\eta f_\tau}{K}\left(1 + \frac{\varepsilon f_c}{K}\cos\vartheta\right), \tag{53}$$

$$\tilde{I} = -\varepsilon^2\frac{\eta f_\tau}{K}, \quad \tilde{J} = \varepsilon, \tag{54}$$

with $b = t^2 + 9\hat{s}^2$.

(iii) *Proof of inflexional disequilibrium*: The set of Eqs. (44)–(46) are re-written as

$$\tilde{A}\chi^2 + \tilde{B} + \tilde{C}\chi = 0, \tag{55}$$

$$\tilde{D}\chi^2 + \tilde{E} + \tilde{F}(\Delta_\theta + \chi\Delta_s) = 0, \tag{56}$$

$$\tilde{G}\chi^2 + \tilde{H}\chi + \tilde{I}(\Delta_\theta + \chi\Delta_s) + 2\tilde{J}(\chi\Delta_\theta + \Delta_s) = 0, \tag{57}$$

in the three unknowns $\chi = B_\theta/B_s$, $\Delta_\theta = (B_s)^{-1}\partial B_\theta/\partial\varepsilon$ and $\Delta_s = (B_s)^{-1}\partial B_s/\partial\varepsilon$. Since $\tilde{C}^2 - 4\tilde{A}\tilde{B} \geqslant 0$ always, we look for two real solutions χ_1 and χ_2 of (55).

This is done by numerical and asymptotic analysis. Numerically, we explore existence of possible solutions in the parameter space given by $\varepsilon \in [0.0001, 0.1]$ and $\eta \in [0, 1.5]$, at different times t, with $\hat{s} \gg |t|$. Since (30) is anti-symmetric in t, without loss of generality we restrict the analysis to $t > 0$. The range of values considered are given by $\hat{s} \in [-1, 1]$ and $t \in [0.0001, 0.1]$, with $\vartheta \in [0, 2\pi]$. Numerical analysis shows (see diagrams of Fig. 4) that χ (and therefore B_θ) blows-up as $\sec\vartheta = 1/\cos\vartheta$ at $\vartheta = \pi/2$ and $3\pi/2$. Hence, there is no real solution to (55) and therefore no equilibrium. Note that the singularity is independent of the flux-tube thickness a/R.

The asymptotic analysis made with respect to ε confirms this result. By taking terms up to the order of ε^2, the functions in (44) reduce to

$$\tilde{A} \sim -\varepsilon\eta f_c f_\tau\cos\vartheta + \varepsilon^2\eta f_c^2 f_\tau\left(3\sin^2\vartheta - \cos^2\vartheta\right), \tag{58}$$

$$\tilde{B} \sim \varepsilon\left(\frac{18\hat{s}}{b^{1/2}}\sin\vartheta - \eta f_c f_\tau\cos\vartheta\right) + \varepsilon^2\eta f_c^2 f_\tau, \tag{59}$$

$$\tilde{C} \sim f_c\cos\vartheta - \varepsilon f_c^2\sin^2\vartheta + \varepsilon^2\left[f_c^3\sin^2\vartheta\cos\vartheta - \frac{18\hat{s}}{b^{1/2}}\eta f_\tau\sin\vartheta - \eta f_c\left(\frac{54t\hat{s}}{b^2}\sin\vartheta - \eta f_\tau^2\cos\vartheta\right)\right], \tag{60}$$

and the solutions (up to terms of order ε) are given by

$$\chi_1 = \frac{\varepsilon}{\cos\vartheta}\left[f_c^3\sin^4\vartheta + 2\eta f_\tau\cos\vartheta\left(\frac{18\hat{s}}{b^{1/2}}\sin\vartheta - \eta f_c f_\tau\cos\vartheta\right)\right] + O(\varepsilon^2), \tag{61}$$

and

$$\chi_2 = \frac{1}{\varepsilon\eta f_\tau} + \frac{f_c}{\eta f_\tau\cos\vartheta}(3\sin^2\vartheta - 1) + \varepsilon\left[\frac{3\sin^2\vartheta - \cos^2\vartheta}{\eta\cos^2\vartheta} - f_c^3\frac{\sin^2\vartheta}{\cos\vartheta}\times(2\cos^2\vartheta + \sin^2\vartheta) + \frac{108t\hat{s}}{b^2}\eta f_c\sin\vartheta\right] + O(\varepsilon^2). \tag{62}$$

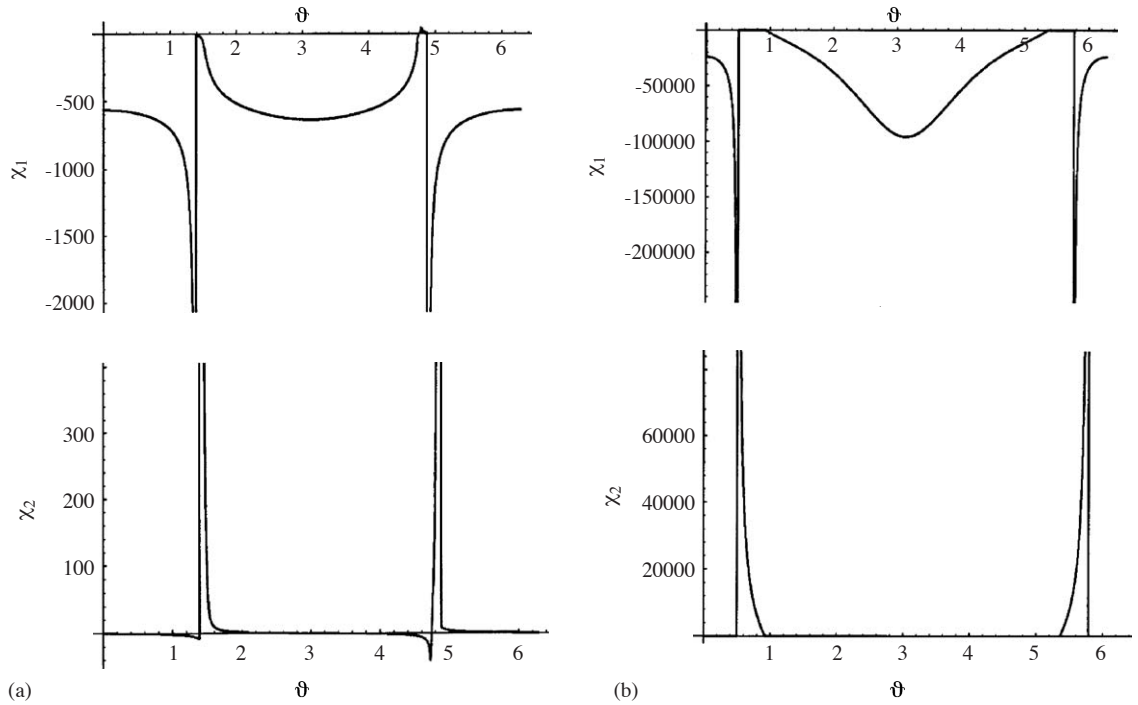

Fig. 4. Examples of solution curves to Eq. (55). The diagrams show χ_1 and χ_2 plotted against ϑ at (a) $\varepsilon = 0.1$ and (b) $\varepsilon = 1$, for $t = 0.001$ and $\eta = 0.5$. The solutions blow-up as $\sec\vartheta = 1/\cos\vartheta$ at $\vartheta = \pi/2$ and $\vartheta = 3\pi/2$. This behaviour, generic and independent of the values of parameters chosen, is confirmed by asymptotic analysis (see Eqs. (61)–(63)).

Both solutions blow-up with $\sec\vartheta = 1/\cos\vartheta$ at $\vartheta = \pi/2$ and $\vartheta = 3\pi/2$. In plane geometry, we have no torsion ($\eta = 0$) and the tube axis has an S-shape, as in Fig. 3a; in this case the solution χ_2 disappears (Eq. (44) becomes linear in χ), but the singularity survives in χ_1. From (61), we have

$$\lim_{\eta\to 0}\ \chi_1 = \varepsilon f_c^3\,\frac{\sin^4\vartheta}{\cos\vartheta}. \tag{63}$$

This proves that $\tilde{\mathscr{K}}_{m,t}$ has no inflexional equilibrium. □

6. Relaxation of inflexional magnetic flux-tubes to inflexion-free configurations

Inflexional disequilibrium has important implications for the ideal relaxation of magnetic flux-tubes and their evolution. Suppose that the flux-tube is in inflexional state at some time t_0. Because of the disequilibrium of the inflexional configuration, there is a rotational flow that induces a local natural rearrangement of the flux-tube strand in $\mathscr{D}$, for $|t| > t_0$. Since in ideal conditions topology is conserved (as a consequence of Cauchy's solutions to Faraday's equation), inflexional geometry is isotoped through a diffeomorphism of the ambient space to an inflexion-free state. Hence, as a consequence of inflexional disequilibrium, we have:

Corollary. *Let $\tilde{\mathscr{K}}_{m,t_0}$ denote a magnetic flux-tube in inflexional disequilibrium. $\tilde{\mathscr{K}}_{m,t_0}$ is naturally isotoped to an inflexion-free state $\mathscr{K}_{m,t}$ in $\mathscr{D}$, for any $|t| > t_0$.*

Relaxation to inflexion-free configuration is attained through local re-arrangement of the tube geometry and field-line distribution. This, in turn, brings a re-distribution of internal energy and writhe and twist helicity. In Section 4, we mentioned that passage through an inflexional state is invariably associated with the exchange of writhe and twist in the flux-tube (see Fig. 3b). In astrophysical flows, though, nature prevents attaining high values of twist, and above a certain threshold of twist value (critical twist) flux-tubes become kink-unstable. Typically, kink instability triggers the eruption of energy from solar coronal loops and confined plasmas. Estimates made on solar coronal loop models, where the contribution from B_θ^2/r is generally small compared with tension effects, indicate (see, for example, Priest et al., 1989) that kink instability takes place at $T w_{\rm cr} \approx 2$ (the exact value depending on the particular geometry and magnetic field distribution); in the case of uniform twist, by using Eq. (27), we have

$$\frac{B_s^2 c/K}{B_\theta^2/r} = \frac{K L^2 c}{(2\pi T w_{\rm cr})^2 r} \propto \frac{K R}{T w_{\rm cr}^2 r} \gg \frac{K}{T w_{\rm cr}^2} = O(1). \tag{64}$$

Below critical twist magnetic flux-tubes, free to move in the ambient space, tend to lower their surplus of net twist by converting torsional energy into bending energy, a process similar to the relaxation of super-twisted elastic strings (and super-coiled DNA) to highly bent configurations (Ricca, 1995). In ideal magnetohydrodynamics, this process is known to convert twist helicity to writhe helicity, and it has clearly important effects on the energy re-distribution of magnetic structures, in the solar corona, in astrophysical flows, and in laboratory plasmas.

Acknowledgements

I wish to thank the Isaac Newton Institute for Mathematical Sciences, Cambridge (UK), for its kind hospitality. Financial support from The Royal Society of London and UK-EPSRC is also kindly acknowledged.

References

Berger, M.A., Field, G.B., 1984. The topological properties of magnetic helicity. J. Fluid Mech. 147, 133–148.

Bray, R.J., Cram, L.E., Durrant, C.J., Loughhead, R.E., 1991. Plasma Loops in the Solar Corona. Cambridge University Press, Cambridge.

Chui, A.Y.K., Moffatt, H.K., 1996. The energy and helicity of knotted magnetic flux tubes. Proc. R. Soc. London A 451, 609–629.

Fuller, F.B., 1971. The writhing number of a space curve. Proc. Nat. Acad. Sci. USA 68, 815–819.

Mercier, C., 1963. Sur une representation des surfaces toroidales: applications aux equilibres magnetohydrodynamiques. Nucl. Fusion 3, 89–98.

Moffatt, H.K., Ricca, R.L., 1992. Helicity and the Călugăreanu invariant. Proc. R. Soc. London A 439, 411–429.

Priest, E.R., Hood, A.W., Anzer, U., 1989. A twisted flux tube model for solar prominences. I. General properties. Astrophys. J. 344, 1010–1025.

Ricca, R.L., 1994. Writhe and twist helicity contributions to an isolated magnetic flux tube and hammock configuration. In: Belvedere, G. et al. (Eds.), VII European Meeting on Solar Physics. Catania Astrophysical Observatory, pp. 151–154.

Ricca, R.L., 1995. The energy spectrum of a twisted flexible string under elastic relaxation. J. Phys. A: Math. Gen. 28, 2335–2352.

Ricca, R.L., 1997. Evolution and inflexional instability of twisted magnetic flux tubes. Solar Phys. 172, 241–248.

Ricca, R.L. (Ed.), 2001. An Introduction to the Geometry and Topology of Fluid Flows. NATO ASI Series II, vol. 47. Kluwer.

Ricca, R.L., Berger, M.A., 1996. Topological ideas and fluid mechanics. Phys. Today 49 (12), 24–30.

Ricca, R.L., Moffatt, H.K., 1992. The helicity of a knotted vortex filament. In: Moffatt, H.K. et al. (Eds.), Topological Aspects of the Dynamics of Fluids and Plasmas. Kluwer Academic Publishers, Dordrecht, The Netherlands, pp. 225–236.